Stereochemically Nonrigid Six-Coordinate Molecules. I. A Detailed Mechanistic Analysis for the Molecule $FeH_2[P(OC_2H_5)_3]_4$

P. Meakin, E. L. Muetterties, F. N. Tebbe, and J. P. Jesson*

Contribution No. 1798 from the Central Research Department, E. I. du Pont de Nemours and Company, Experimental Station, Wilmington, Delaware 19898. *Received February 4, 1971*

Abstract: Analysis of the ^1H and ^{31}P nmr data for $FeH_2[P(OC_2H_5)_3]_4$ over a temperature range encompassing slow- and fast-exchange limits characterizes this molecule as stereochemically nonrigid on the nmr time scale. The nmr line-shape changes for the complex $AA'X_2YY'$ spin system have been treated in first-order and in complete form. Abstract mechanistic analysis was performed in terms of the point group of the molecule and the possible nuclear permutations to determine the distinguishable basic sets of permutations. The observed line shapes were then compared with line shapes calculated for each of the sets. Only one of the four basic sets gave simulated line shapes in agreement with experiment. $FeH_2[P(OC_2H_5)_3]_4$ in the solid state has a phosphorus atom spatial distribution closer to a tetrahedral array than to octahedral coordination sites. This information, together with ancillary data, suggests that the most reasonable physical model consistent with the assigned basic permutations consists of a process in which the hydrogen atoms traverse the face positions of an approximately regular tetrahedral arrangement of phosphorus ligands. The only physical model previously considered for stereochemically nonrigid six-coordinate complexes is the trigonal twist. A concerted mechanism based on this model is rigorously excluded as a dominant rearrangement mechanism in $FeH_2[P(OC_2H_5)_3]_4$.

In two preliminary communications[1,2] we outlined evidence for stereochemical nonrigidity in a class of six-coordinate hydrides of the form H_2ML_4. A novel rearrangement mechanism was proposed to which we have assigned the descriptive label "tetrahedral tunneling." (We do not necessarily imply quantum mechanical tunneling.) In presenting the complete body of experimental and theoretical data, there will be several articles: (1) this, the first in the series, which treats in detail the nmr data for the molecule $FeH_2[P(OC_2H_5)_3]_4$ and defines the basic permutational scheme for the rearrangement, showing that it corresponds to the permutations required for "tetrahedral tunneling"; (2) a full X-ray crystal structure presentation for *cis*-$FeH_2[C_6H_5P(OC_2H_5)_2]_4$[3,4] and for *trans*-$RuH_2[C_6H_5P(OC_2H_5)_2]_4$;[5] (3) nuclear resonance data and analysis for some 20 H_2ML_4 complexes; (4) the synthesis and chemical properties of these hydrides; and (5) analysis of the HML_4 family for which a rearrangement mechanism of the "tetrahedral tunneling" type is likely.

This first article shows that there are only four possible basic permutational sets, of which only one gives the correct simulated line-shape behavior with temperature. A variety of physical models is considered, both for the experimentally established permutation and for the other permutational schemes.

(A) Experimental Section

$FeH_2[P(OC_2H_5)_3]_4$ was prepared by sodium borohydride reduction of a triethyl phosphite–iron(II) iodide solution in ethanol.

Nmr samples in toluene-d_8 were prepared in a nitrogen atmosphere. Proton nmr spectra were run over the temperature range -50 to $+85°$, using Bruker HFX-90 and Varian HR-220 spectrometers. ^{31}P spectra (36.43 MHz) were observed over the same temperature range, with and without proton noise decoupling, using the Bruker spectrometer. The ^{31}P samples were run in 10-mm tubes, and field-frequency stabilization was achieved using the fluorine signals from 1,2-dibromotetrafluoroethane or C_6F_6 coaxial capillaries, depending on the temperature range.

Temperatures for the spectra from the HR-220 were measured by observing the chemical shift separation in methanol or ethylene glycol samples run before and after each trace. For the HFX-90, temperatures were measured with a copper–constantan thermocouple located just below the sample tube and were calibrated using a similar thermocouple held coaxially in the spinning sample tube.

(B) Stereochemical Nonrigidity in $FeH_2[P(OC_2H_5)_3]_4$

The slow-exchange limit 220- and 90-MHz ^1H hydride spectra for $FeH_2[P(OC_2H_5)_3]_4$ are shown in the first lines of Figures 1 and 2, respectively. Using the nuclear labeling system shown in Figure 3, these low-temperature-limit spectra were simulated using the following nmr parameters.

$$J_{15} = J_{16} = J_{25} = J_{26} = 66.5 \text{ Hz}$$

$$J_{13} = J_{14} = J_{23} = J_{24} = 56.0 \text{ Hz}$$

$$\begin{Bmatrix} J_{36} = J_{45} \\ J_{35} = J_{46} \end{Bmatrix} = \begin{Bmatrix} 24 \text{ Hz} \\ -6 \text{ Hz} \end{Bmatrix}$$

$$J_{56} = -5 \text{ Hz} \qquad J_{34} \sim 0 \text{ Hz}$$

$$\tau = 23.86\ (30°) \qquad \delta_{34} - \delta_{12} = 2.2 \text{ ppm}^{6}\ (-70°)$$

The coupling constants which could not be determined directly from the spectra (those with values <20 Hz) were estimated by finding the values which gave a best visual fit to the observed spectra. The fits to the two sets of spectra in the low-temperature limit are shown in the first rows of Figures 1 and 2.

(1) F. N. Tebbe, P. Meakin, J. P. Jesson, and E. L. Muetterties, *J. Amer. Chem. Soc.*, **92**, 1068 (1970).

(2) P. Meakin, L. J. Guggenberger, J. P. Jesson, D. H. Gerlach, F. N. Tebbe, W. G. Peet, and E. L. Muetterties, *ibid.*, **92**, 3432 (1970).

(3) L. J. Guggenberger, D. D. Titus, M. T. Flood, R. E. Marsh, A. A. Orio, and H. B. Gray, *ibid.*, in press.

(4) We are presently trying to obtain single crystals of the trans isomer to compare the distortions with those for the cis molecule and with those for *trans*-$RuH_2[C_6H_5P(OC_2H_5)_2]_4$.

(5) L. J. Guggenberger, manuscript in preparation.

(6) The temperature dependence of the chemical shift separation is ~ -0.1 Hz/deg at 36.43 MHz.

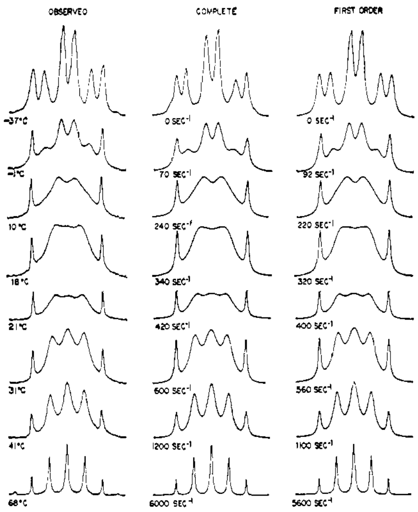

Figure 1. Observed and calculated 220-MHz ^{1}H hydride nmr spectra of $FeH_2[P(OC_2H_5)_3]_4$ as a function of temperature. The results are shown for first-order and complete calculations using the basic permutational set IV.

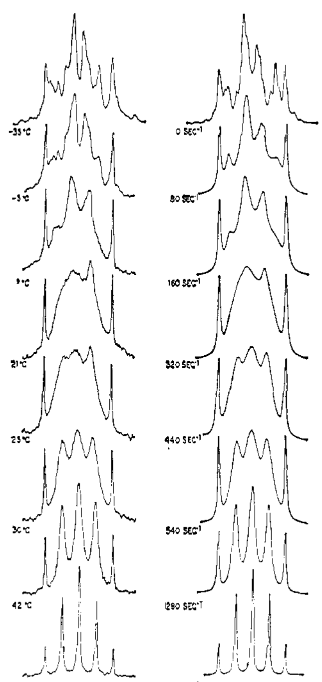

Figure 2. Observed and calculated 90-MHz ^{1}H hydride nmr spectra for $FeH_2[P(OC_2H_5)_3]_4$. The calculated spectra are for the basic permutational set IV.

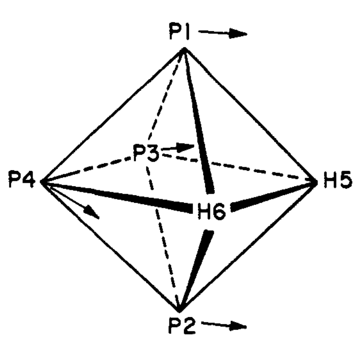

Figure 3. Nuclear labeling scheme and distortion from idealized octahedral geometry for *cis*-H_2ML_4 molecules.

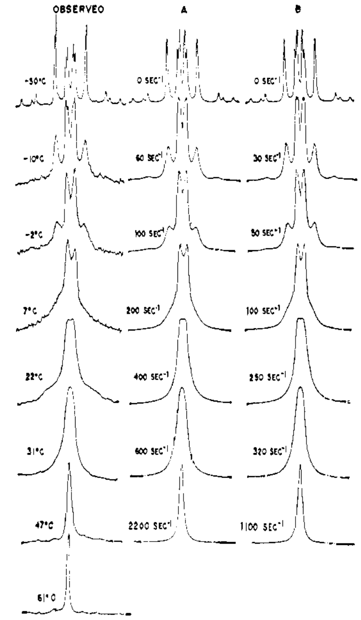

Figure 4. Proton-noise-decoupled ^{31}P (36.4 MHz) spectrum for $FeH_2[P(OC_2H_5)_3]_4$ over a range of temperature together with simulated spectra for the basic permutational sets A and B.

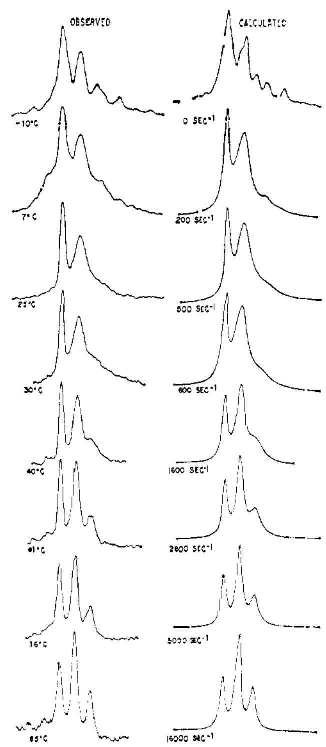

Figure 5. Observed and calculated ^{31}P (36.4 MHz) nmr spectra of $FeH_2[P(OC_2H_5)_3]_4$ as a function of temperature. The calculated spectra are for the basic permutational set IV.

The phosphorus–phosphorus coupling constants, J_{13}, etc., and the phosphorus chemical shifts were obtained from the proton-noise-decoupled ^{31}P spectra which are shown, together with simulated spectra, in Figure 4.

Calculated and observed ^{31}P spectra without proton decoupling are shown in Figure 5.[7]

(7) An attempt was made to vary the nmr parameters systematically to give a best least-squares agreement between calculated and observed

The temperature dependence of the nmr spectra is not detectably altered by variation of concentration or of solvent or by the addition of excess triethyl phosphite. These observations argue against bimolecular or solvent-assisted processes.[8] The fast-exchange ^1H and ^{31}P spectra (Figures 1, 2, and 5) consist of a quintet and a triplet, respectively, with the proper binomial distribution to define spectroscopic equivalence in the hydrogen and phosphorus spin systems. Spin correlation is maintained and stereochemical nonrigidity is therefore established for $FeH_2[P(OC_2H_5)_3]_4$.[9,10]

(C) Mechanistic Analysis. The Basic Permutation Sets

Analysis of the nmr line-shape changes due to exchange, assuming a "jump model," gives information concerning the nuclear permutations which convert the initial labeled configuration into the configuration after rearrangement. No direct mechanistic information is obtained to indicate the actual physical path involved. All routes leading to the correct permutational change are equally acceptable, and one must appeal to other physical-chemical evidence to decide between the possibilities. In this section, we discuss the basic permutational sets that are distinguishable by the nmr technique. In succeeding sections, we describe the method of calculation, assign the permutational sets which will simulate the correct experimental behavior, and establish the actual mechanism for the exchange.

The possible permutations which convert a "labeled" *cis*-$FeH_2[P(OC_2H_5)_3]_4$ molecule into all other possible labeled *cis*-$FeH_2[P(OC_2H_5)_3]_4$ molecules comprise a group of order $4! \times 2!$, *i.e.*, the product of all permutations of the phosphorus nuclei among themselves and all possible permutations of the hydrogens among themselves. These 48 permutations correspond to 48 configurations, with many equivalences.[11]

Using the numbering in Figure 3, the operations or permutations relating equivalent configurations and their cyclic representations in this molecule (C_{2v} point group) are

$$E \begin{pmatrix}123456\\123456\end{pmatrix} = (1)(2)(3)(4)(5)(6)$$

$$C_2 \begin{pmatrix}123456\\214365\end{pmatrix} = (12)(34)(56)$$

$$\sigma_v \begin{pmatrix}123456\\213456\end{pmatrix} = (12)(3)(4)(5)(6)$$

$$\sigma_v' \begin{pmatrix}123456\\124365\end{pmatrix} = (1)(2)(34)(56)$$

spectra using digitized spectral data, but this was unsuccessful. The normal nmr programs cannot be used since only an envelope is observed for the spectrum. (The proton spectrum consists of 84 transitions with 4 degeneracies, and the non-noise-decoupled ^{31}P spectrum consists of 108 transitions with no degeneracies.) Individual transitions cannot be assigned.

(8) We acknowledge possibilities such as "collision" bimolecular processes and "collision" solvent assistance which could be insensitive to the variations discussed.

(9) E. L. Muetterties, *Inorg. Chem.*, 4, 769 (1965).

(10) E. L. Muetterties, *J. Amer. Chem. Soc.*, 90, 5097 (1968).

(11) The term is used to denote configurations related by the operations of the point group of the molecule.

Thus, in this case, there are $^{48}/_4 = 12$ unique Hamiltonians for the spin system. Nmr line shapes are only affected by permutations which exchange different spin Hamiltonians.

A basic set of permutations can be generated in the following way. Choose one of the 48 permutations; all permutations that are the transform of the chosen permutation under the symmetry operations of the point group of the molecule must occur with equal rates. A "basic set of permutations" is defined as a set of symmetry-related permutations occurring with the same rate. Having determined a basic set in this way, there will be three other equivalent basic sets which can be generated by applying the operators C_2, σ_v, σ_v' successively to the original set. Any one of these four sets or any linear combination of them gives rise to the same calculated line shapes. Next, one of the 48 permutations not already generated in the above process is chosen and the procedure is repeated until all 48 permutations are accounted for. We find that there are four sets of basic permutations, in addition to the permutations corresponding to the point group C_{2v}, and they may be written as follows.

$$E \quad (1)(2)(3)(4)(5)(6)$$

$$\text{I} \quad \begin{pmatrix}123456\\341256\\432156\end{pmatrix} = \begin{matrix}(13)(24)\\(14)(23)\end{matrix}$$

$$\text{II} \quad \begin{pmatrix}123456\\124356\end{pmatrix} = (34)$$

$$\text{III} \quad \begin{pmatrix}123456\\134256\\142356\\324156\\421356\end{pmatrix} = \begin{matrix}(234)\\(243)\\(134)\\(143)\end{matrix}$$

$$\text{IV} \quad \begin{pmatrix}123456\\321456\\132456\\143256\\423156\end{pmatrix} = \begin{matrix}(13)\\(23)\\(24)\\(14)\end{matrix}$$

These permutation sets and the corresponding equivalent sets generated by applying the C_2, σ_v, and σ_v' operations comprise the 48 elements of the molecular permutation group for the FeH_2P_4 skeleton. Reference will be made to a permutation set V which corresponds to random exchange and consists of all group permutations equally weighted.

The I–IV notation will be retained in the following discussion to label the experimentally distinguishable types of line-shape behavior based on the jump model. In the exchange calculations, the exchange rates are defined as the rates at which one configuration is transformed to any other configuration.

For the analysis of the A_2B_2 phosphorus spin system of $FeH_2[P(OC_2H_5)_3]_4$ (proton-noise-decoupled spectra) the permutational group is of order $4! = 24$. There are six unique Hamiltonians and three distinguishable sets of permutations, E and two sets (A and B) which effect Hamiltonian exchange. The basic sets are

E (1)(2)(3)(4)(5)(6) $\times$ $[(E)(C_2)(\sigma_v)(\sigma_v')]$

A (13)
(23)
(24) $\times$ $[(E)(C_2)(\sigma_v)(\sigma_v')]$
(14)

B (13)(24) $\times$ $[(E)(C_2)(\sigma_v)(\sigma_v')]$

The previous permutational sets I–IV correspond to the sets in this subgroup as follows: II and E with E, I with B, and III and IV with A. The four basic, distinguishable permutational sets I–IV have now been defined. Any exchange mechanism will correspond to either one or to a linear combination of basic permutational sets.

(D) Line-Shape Calculations

The line-shape calculations in this paper employ the density-matrix approach of Kaplan[12] and Alexander.[13] This method together with the theories of Redfield[14] and of Sack[15] has been applied to a variety of nmr problems over the last 10 years. However, only recently, with the advent of the numerical techniques developed by Gordon and McGinnis,[16] Binsch,[17] and Schirmer, Noggle, and Gaines[18] has it become possible to treat spin systems of any complexity. Utilization of symmetry factoring increases the scope of the method further, and in the present approach, X, magnetic equivalence and point group symmetry factoring are achieved for the AA'X$_2$YY' spin system using numerical techniques. Analytical factoring is perhaps more elegant but is difficult to apply with any generality.[19]

The phenomenological density matrix equation of motion is[13,20]

$$\frac{d\rho}{dt} = 2\pi i[\rho, H] + \left(\frac{d\rho}{dt}\right)_{\text{relax}} + \sum_i (P_i^+\rho P_i + P_i\rho P_i^+ - 2\rho)/2\tau_i \quad (1)$$

where ρ is the mean spin density matrix, H is the mean spin Hamiltonian including interaction with the radiofrequency field, and $(d\rho_{ij}/dt)_{\text{relax}} = -\rho_{ij}/T_2$ for the density matrix elements one off diagonal in I_z, T_2 being a relaxation time which determines the line width in the absence of exchange. The P_i's are exchange matrices defined by $\Psi'(t) = P_i\Psi(t)$, where $\Psi(t)$ and $\Psi'(t)$ are the spin wave functions before and after the exchange process. τ_i is the average time between exchanges of the ith type.

In the appropriate Liouville space, eq 1 can be written as[17,21,22]

$$d\boldsymbol{\rho}/dt = -i\mathcal{L}\boldsymbol{\rho} + \mathbf{R}\boldsymbol{\rho} + \sum_i \chi_i\boldsymbol{\rho} \quad (2)$$

where $\boldsymbol{\rho}$ is now the density vector in Liouville space, $\mathcal{L}$ is the Liouville operator, $\mathbf{R}$ is the relaxation operator, and the χ_i's are the exchange operators. The absorption intensity in the absorption mode is proportional to the imaginary parts of the transverse component of the complex magnetization in a coordinate system rotating with angular velocity $\omega = 2\pi\nu$, where ν is the frequency of the radiofrequency field and is given by

$$I(\omega) \propto \text{Im}(\boldsymbol{\rho}^{\omega}\cdot\mathbf{M}^-) = \text{Im}(\mathbf{M}^-\cdot\boldsymbol{\rho}^{\omega}) \quad (3)$$

where $\boldsymbol{\rho}^{\omega}$ is the density vector in the rotating frame and $\mathbf{M}^- = \Sigma_i\gamma_i\mathbf{I}_i^-$, $\mathbf{I}_i^-$ being a vector containing the matrix elements of the spin-lowering operator for the ith nucleus.

Under the conditions normally assumed in nmr line-shape analysis, slow passage, high temperature, and weak radiofrequency fields, eq 2 and 3 give the line-shape expression

$$I(\omega) \propto -\text{Re}\{\mathbf{M}^-\cdot[\sum_i\chi_i + \mathbf{R} - i\mathcal{L}_0(\omega)]^{-1}\cdot\mathbf{M}^-\} \quad (4)$$

where $\mathcal{L}_0(\omega)$ is the Luoiville operator corresponding to the high-resolution nmr Hamiltonian H_0 excluding the interaction with the radiofrequency field. The direct use of eq 4 necessitates a matrix inversion at each frequency ν needed to construct a plot of the calculated spectra (typically 500–1000 points in our calculations). To avoid point-by-point matrix inversion, we exploit the fact that eq 4 has the form[16–18]

$$I(\omega) \propto -\text{Re}[\mathbf{M}^-\cdot(\mathbf{A}_0 - \mathbf{E}i\omega)^{-1}\cdot\mathbf{M}^-] \quad (5)$$

where $\mathbf{A}_0$ is a constant complex non-Hermitian matrix and $\mathbf{E}$ is the unit matrix. Thus the transformation that diagonalizes $\mathbf{A}_0$ diagonalizes $(\mathbf{A}_0 - \mathbf{E}i\omega)$ at all frequencies and the evaluation of $I(\omega)$ involves only the inversion of a diagonal complex matrix and the calculation of the product of a complex vector containing the diagonal elements of the inverted matrix with a second constant vector whose elements are given by

$$\mathbf{S}_i = (\mathbf{M}^-\cdot\mathbf{T})_i(\mathbf{T}^{-1}\cdot\mathbf{M}^-)_i \quad (6)$$

when $\mathbf{T}$ is the transformation that diagonalizes $\mathbf{A}_0$

$$\mathbf{T}^{-1}\mathbf{A}_0\mathbf{T} = \Lambda \quad (7)$$

For the present six-spin system, the appropriate Liouville space has dimension 4096 $\times$ 4096. However, for weak radiofrequency fields, only elements of the density matrix one off diagonal in I_z (single quantum transition) need be considered. The high-resolution nmr Hamiltonian and exchange matrices P_i are diagonal in I_z and this, together with the simple diagonal form assumed for the relaxation operator $\mathbf{R}$, permits factorization of (4) into six equations, the largest of which has dimension 300 $\times$ 300 corresponding to the $I_z = 0 \rightarrow 1$ and $I_z = -1 \rightarrow 0$ transitions. X factoring of the different nuclear types (^{1}H and ^{31}P) allows consideration of only density matrix elements one off diagonal in $I_{z\text{P}}$ or one off diagonal in $I_{z\text{H}}$. The largest complex non-Hermitian matrices are thereby reduced to 72 $\times$ 72 for the proton transitions and 96 $\times$ 96 for the ^{31}P transitions.

Point group symmetry and magnetic equivalence allow further factoring. In the basis in which the

(12) J. I. Kaplan, *J. Chem. Phys.*, **28**, 278 (1958); **29**, 462 (1958).
(13) S. Alexander, *ibid.*, **37**, 967, 974 (1962); **38**, 1787 (1963); **40**, 2741 (1964).
(14) A. G. Redfield, *IBM J. Res. Develop.*, **1**, 19 (1957); *Advan. Magn. Resonance*, **1**, 1 (1965).
(15) R. A. Sack, *Mol. Phys.*, **1**, 163 (1958).
(16) R. G. Gordon and R. P. McGinnis, *J. Chem. Phys.*, **49**, 2455 (1968).
(17) G. Binsch, *J. Amer. Chem. Soc.*, **91**, 1304 (1969).
(18) R. E. Schirmer, J. H. Noggle, and D. F. Gaines, *ibid.*, **91**, 6240 (1969).
(19) D. A. Kleier and G. Binsch, *J. Magn. Resonance*, **3**, 146 (1970).

(20) We restrict our discussion to the case of mutual exchange.

(21) U. Fano in "Lectures on the Many Body Problem," Vol. 2, E. R. Caianiello, Ed., Academic Press, New York, N. Y., 1964, p 217.

(22) Boldface type is used to denote vectors, matrices, and operators (superoperators) in Liouville space. $\mathcal{L}$ is the Luoiville operator; χ_i's are exchange operators.

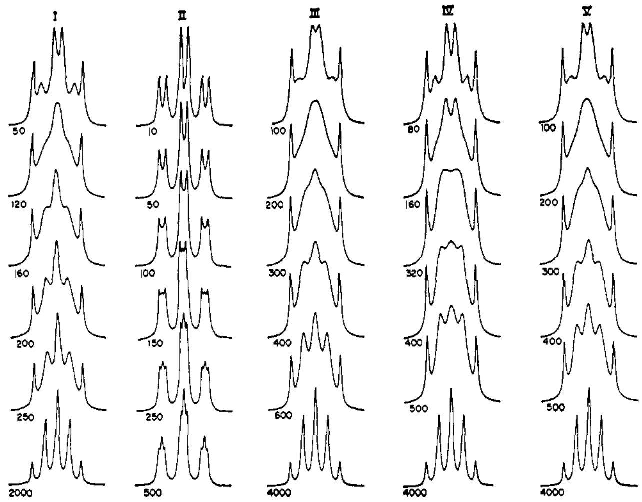

Figure 6. Calculated first-order line shapes as a function of exchange rate for mechanisms I–IV discussed in section C, together with a calculation for random exchange (V). The exchange rates are in units of sec^{-1}.

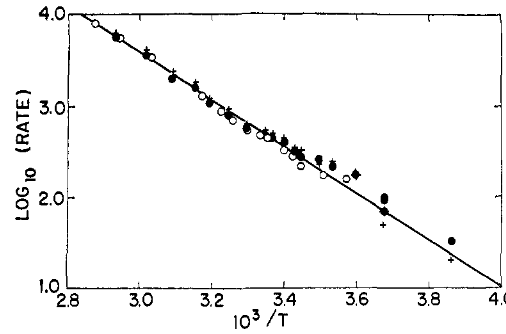

Figure 7. Arrhenius plot for rate data obtained from 220- and 90-MHz ^1H nmr data for $FeH_2[P(OC_2H_5)_3]_4$: (○) 90-MHz spectra, complete calculation; (+) 220-MHz spectra, complete calculation; (●) 220-MHz spectra, first-order calculation.

Hamiltonian is diagonal there is a one-to-one correspondence between the density matrix elements and the transitions so that, if the exchange processes have the symmetry implied by the form of the Hamiltonian, the largest matrices that need to be diagonalized are of dimension 20 × 20 for the ^1H and 28 × 28 for the ^{31}P transitions. (Only density matrix elements corresponding to allowed transitions need be considered. See Appendix II). These represent maximum sizes, the actual sizes depending on the specific permutations involved in the exchange.

A general computer program has been written for the case of mutual exchange based on the formalism outlined above. The I_z factoring is carried out explicitly; the X factoring, point group symmetry factoring, and magnetic equivalence factoring are carried out using numerical procedures. Some features of the program are described in Appendix I. In cases where the nmr spectra are first order, considerable further simplification is possible and the above approach reduces to the equation given by Sack.[15] A separate program has been written which takes advantage of these simplifications.

(E) Mechanism. Permutational Distinctions

(1) Proton Nmr. The first column of Figure 1 shows the observed 220-MHz ^1H hydride spectrum of $FeH_2[P(OC_2H_5)_3]_4$ as a function of temperature. The two outer lines in the spectrum, which remain sharp at all temperatures, correspond to transitions $|H(\alpha\alpha);\ P(\alpha\alpha\alpha\alpha)\rangle \rightarrow |H(\alpha\beta + \beta\alpha);\ P(\alpha\alpha\alpha\alpha)\rangle$ and $|H(\alpha\beta + \beta\alpha);\ P(\alpha\alpha\alpha\alpha)\rangle \rightarrow |H(\beta\beta);\ P(\alpha\alpha\alpha\alpha)\rangle$ for one of the lines and corresponding functions with $P(\beta\beta\beta\beta)$ for the other line. These transitions are clearly unaffected by any of the permutations and therefore provide a direct measure of the line width in the absence of exchange. As implied by the form of the density-matrix equations discussed above, all line widths in the absence of exchange are assumed to be the same. The ability to measure T_2 directly in this manner allows calculations of accurate exchange data for faster exchange rates than would otherwise be possible.

Using the spectral parameters outlined in section B, the line-shape behavior was calculated as a function of exchange rate for each of the basic permutational schemes (I–IV) discussed in section C. The calculations were performed in the first-order approximation, and the results are shown in Figure 6 together with a set of results for random exchange (all permutations in mechanism I–IV equally likely, column labeled V). Mechanism II does not average the phosphorus environments, so the high-temperature limit is a triplet of triplets rather than the experimentally observed quintet. All the other mechanisms give the correct high-temperature-limit behavior. Cases III and V give similar, although not identical, line-shape results. Only mechanism IV gives results in close agreement with experiment.

Similar first-order calculations for combinations of the mechanisms I–IV have been carried out. The only combinations which can be made to give reasonable agreement with experiment contain predominantly mechanism IV. Fits for the 220-MHz ^1H spectra using permutational scheme IV are shown for first-order and complete calculations, together with the observed spectra, in Figure 1. The procedure used was to determine T_2 from the width of the outer lines and to vary the exchange rate until the best visual agreement was obtained between the observed and calculated spectra. It is clear that the first-order treatment is adequate for these spectra. By contrast, the 90-MHz ^1H hydride spectra are quite asymmetric and cannot be fit using a first-order treatment; the complete treatment, on the other hand, gives good agreement, the observed and simulated (permutation set IV) spectra being shown in Figure 2.

Exchange rates obtained from the 220- and 90-MHz spectra are presented as an Arrhenius plot in Figure 7. The straight line corresponds to the rate expression

$$R(T) = 10^{11.3}e^{-11700/RT}$$

Alternatively, the temperature dependence of the rate can be expressed in terms of the Eyring equation

$$R(T) = K(kT/h)e^{-\Delta G^{\ddagger}/RT}$$

and the activation parameters are

$$\Delta G^{\ddagger}(298°) = 13,700 \text{ cal mol}^{-1}$$

$$\Delta H^{\ddagger}(298°) = 11,100 \text{ cal mol}^{-1}$$

$$\Delta S^{\ddagger}(298°) = -8.8 \text{ cal mol}^{-1}\text{ deg}^{-1}$$

assuming the transmission coefficient $K = 1$.

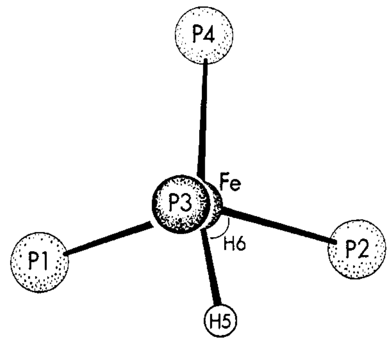

Figure 8. Phosphorus–hydride–iron skeleton of $FeH_2[P(OC_2H_5)_2C_6H_5]_4$ taken from X-ray crystal structure data.[3] The perspective looking down the P3–Fe–H6 axis was chosen to illustrate the postulated exchange mechanism. Phosphorus atoms P1, P2, P4 are in a nearly trigonal array about this axis and the mechanism involves the motion of H5, which is in the face between P1, P2, and P3, into the face between P1, P4, and P3 or between P2, P3, and P4. An essentially identical perspective could have been drawn looking down the P4–Fe–H5 axis to show the single hydrogen step for H6.

The Arrhenius activation energy of 11.7 kcal mol^{-1} is closely related to, but not identical with, the barrier to the intramolecular exchange process.[23] In most cases the discrepancy is small. If the reduced mass (moment of inertia) for the exchange process is small, quantum tunneling may provide lower energy reaction paths, and this effect combined with the correction for the zero-point energy may result in an Arrhenius activation energy somewhat smaller than the barrier height. In the present case, we believe that the exchange process involves mainly motion of the hydrogen atoms; however, it is clear from the X-ray crystal structure data that there must be appreciable motion of the phosphorus nuclei during the rearrangement. This is the major contribution to the reduced mass for the process. The various effects are difficult to estimate, but the difference between the barrier height and the Arrhenius activation energy is probably less than 1 kcal mol^{-1}.

(2) **^{31}P Spectra.** In Figure 4, the proton-noise-decoupled ^{31}P spectrum of $FeH_2[P(OC_2H_5)_3]_4$ is shown as a function of temperature together with spectra simulated on the basis of the permutation schemes A and B outlined in section C. The spectra calculated in this way for the two mechanisms, although not identical, are so similar that no definitive mechanistic distinction can be established. A comparison has also been made between observed and calculated ^{31}P spectra without noise decoupling (Figure 5). With the exception of the sets corresponding to case II, which give an incorrect high-temperature limit, simulated line shapes for different basic permutations are very similar because much of the detail is obscured by overlap of the spectral lines and small couplings to the ligand protons. Thus only one set is presented in the diagram (mechanism IV). No attempt was made to produce accurate fits to the ^{31}P spectra since they provide no additional mechanistic information.

(F) Mechanism. Physical Models

Of the four basic permutational sets (I–IV) only the sets of type IV give line shapes in good agreement with experiment. Since the calculations are based on the jump model, the information obtained consists only of which nuclei are interchanged during the exchange process and contains nothing about how the exchange process occurs. The results do, however, exclude as predominant any physical mechanisms which would give rise to permutations in the sets I, II, and III. To obtain more information on the physical details other approaches must be adopted. For example, a detailed analysis of the infrared and Raman spectra could provide a description of the molecular force field to permit distinction between possible mechanisms. The application of this method is, however, difficult in practice and is not pursued here.

Indirect information was obtained from a study of the variation of the barrier to exchange with changes in molecular structure and from studies of structural details using single-crystal X-ray techniques. In $FeH_2[C_6H_5P(OC_2H_5)_2]_4$ the four phosphorus atoms are arranged in a configuration that corresponds more closely to regular tetrahedral than to idealized octahedral coordination positions; the structure can be described as a tetrahedron with the hydrogens located in two of the faces.[3] This structure suggests a mechanism for exchange consisting of the passage of the hydrogens from one face to another *via* a tetrahedral edge (Figure 8). The permutations required for this mechanism, assuming motion of a single hydrogen, do, in fact, correspond to mechanism IV. Similarly, the increase in barrier on going from iron to ruthenium as central atom is consistent with decreased steric push toward a regular tetrahedron due to increased metal covalent radius. Some crude correlation is also obtained between ligand cone angle[24] and barrier for some metal dihydrides, *suggesting* that the greater the steric push the lower the barrier. However, this is a gross oversimplification and has some validity only when the ligands to be compared are symmetrically substituted and do not differ electronically. Another note of caution must be injected here. Although it is reasonable that the contribution of phosphorus skeletal rearrangement to the barrier should decrease with bulkier ligands, it is also possible that the physical bulk of ligand atomic material along the path the hydrogen would traverse could raise the hydrogen motion contribution to the barrier.

A concerted trigonal or Bailar twist[10] mechanism is ruled out since the permutations involved do not correspond to mechanism IV. A PPP twist corresponds to the set of permutations III, and a PPH twist to the set of permutations I. A combination of permutations I and III gives no better agreement than the separate sets.

In a tetrahedral tunneling process, the trans structure could constitute either a transition state or a short-lived intermediate. In fact, the trans molecule is a stable entity for H_2ML_4 complexes with L = $C_6H_5P(OC_2H_5)_2$, $C_6H_5P(OCH_3)_2$ and M = Fe, Ru, there being an equilibrium mixture of the cis and trans species in solution for these cases.[2] A concerted process in which the hydrogens move simultaneously from faces of the phosphorus tetrahedron to edges (the trans transition state) and on to previously unoccupied faces can be ruled out, since this corresponds to permutation set I. A mechanism in which the trans molecule occurs as a

(23) M. Menzinger and R. Wolfgang, *Angew. Chem., Int. Ed. Engl.*, **8**, 438 (1969).

(24) C. A. Tolman, *J. Amer. Chem. Soc.*, **92**, 2956 (1970).

short-lived intermediate and where the hydrogens can move both to previously occupied and previously unoccupied tetrahedral faces can be subdivided into two cases depending on the rate of inversion of the phosphorus framework in the distorted trans structure.[1] If the inversion is rapid relative to the lifetime of the trans intermediate, the process corresponds to the combination of basic permutations $2 \times E + 2 \times \mathrm{I} + 2 \times \mathrm{II} + \mathrm{III} + \mathrm{IV}$. This mechanism can also be ruled out since line shapes calculated for this set do not agree with experiment. If, on the other hand, inversion of the trans intermediate is slow relative to its lifetime, we have the combination of basic mechanisms $2 \times E + \mathrm{I} + \mathrm{IV}$. This set is predominantly IV, and reasonable agreement with experiment can be obtained. Further delineation of this attractive two-step alternative to the mechanism involving single hydrogen motion will require experimental information regarding the rate of inversion of a trans complex.

An analogous "tetrahedral tunneling" mechanism is a realistic alternative to the Berry[25] mechanism for a class of five-coordinate hydrides of the type HML_4. We[26] have found representative members of this class to be stereochemically nonrigid. Expectedly, the barriers are substantially lower than for the six-coordinate class, *e.g.*, the $\Delta G^{\ddagger}$ values for $HRh[P(OC_2H_5)_3]_4$ and for $HM(PF_3)_4$ (Co, Rh, and Ir) and $HM(PF_3)_4^-$ (Ru, Os) fall in the range 5–10 kcal mol^{-1}. The limiting slow-exchange spectra are consistent with a metal coordination in which three phosphorus nuclei are coplanar, with mutually trans hydrogen and phosphorus nuclei on the threefold axis. In fact, structural studies of three HML_4 complexes have established this stereochemistry for the solid state.[27–29] Since the ML_4 substructure is a nearly regular tetrahedron in these HML_4 species, the low rearrangement barriers, relative to those for H_2ML_4 whose ML_4 substructure departs significantly from regular tetrahedral, are explicable.[30]

Conclusion

Nmr line-shape studies in which Arrhenius parameters for the exchange process have been determined are common; studies in which detailed information has been obtained concerning the mechanism of the exchange process are rare. Two recent examples deal with the molecules $(CH_3)_2NPF_4$[31] and $B_2H_5N(CH_3)_2$.[18] The present case represents by far the most complex spin system yet treated in detail and illustrates the power of a systematic analysis of the basic permutations to classify and eliminate mechanistic possibilities. A general computer program has been written to find the basic permutational sets given the generators of the point group of the molecule. The question of systematic permutational analysis and the identification of cases where mechanistic information can be expected from an nmr study will be pursued in a separate publication. The dimensions of the overall mathematical problem for the present case were such that they could not be handled by existing calculational approaches; the numerical factoring techniques outlined in section D and in Appendix I were necessary to make the calculation feasible.

In contradistinction to five-coordinate complexes for which stereochemical nonrigidity is a well-established and frequently observed phenomenon, the class of H_2ML_4 complexes under discussion is the only established example of nonrigidity for six-coordination. We have proposed a novel mechanism for the rearrangement process in which a single hydrogen moves from one face of an approximately tetrahedral array of phosphorus ligands to another unoccupied face across an edge of the tetrahedron, with the remaining hydrogen essentially fixed. This mechanism is the only simple chemically feasible concerted process that produces the nuclear permutations which correspond to the correct line-shape behavior. An acceptable and attractive alternative is a distorted trans *intermediate* of appreciable lifetime.

Acknowledgment. We wish to acknowledge the assistance of G. Watunya and F. W. Barney in obtaining some of the nmr spectra.

Appendix I. Calculation Details

In order to take advantage of symmetry, magnetic equivalence, and X factoring, the following procedure is used.

The first step is to set up and diagonalize the blocks of the Hamiltonian H_0 for $I_z = -I$ and $I_z = -I + 1$. The simple products of eigenfunctions of the z components of angular momentum for the individual spins are used as an initial basis. The matrices which diagonalize the $I_z = -I$ and $I_z = -I + 1$ blocks of the Hamiltonian are then used to transform the appropriate parts of the transition matrix I^-, which has elements one off diagonal in I_z, and of the exchange matrices P_i and P_i^+ (eq 1) to the basis in which the Hamiltonian H_0 is diagonal. Implicitly, the basis of the density matrix ρ has also been changed. In this new basis, the Liouville operator $\mathfrak{L}_0$ and the relaxation operator $\mathbf{R}$ are both diagonal, so density matrix basis elements needed to calculate $I(\omega)$ from eq 3 are connected only by the exchange term $\Sigma_i \chi_i$. The next step is to search the elements of the $I_z = -I$, $I_z = -I + 1$ block of the new transition matrix, now in the energy representation, until an element with magnitude greater than a specified small quantity is located (*i.e.*, until a transition of nonzero intensity is found). The indices i and j of the element I_{ij}^- and its value are stored. These indices also serve to label the corresponding density matrix element ρ_{ij}. The elements of the density matrix connected to ρ_{ij} through the exchange term in eq 1 are found by examining the elements of P_i and P_i^+. The indices of the newly found elements of the density matrix and the value of the corresponding matrix element of I^- are in turn stored and examined for further connections. This process is continued until no further elements can be found. At this stage the matrix elements of I^- that have been found are set equal to zero so that they will

(25) R. S. Berry, *J. Chem. Phys.*, **32**, 933 (1960).

(26) P. Meakin, J. P. Jesson, F. N. Tebbe, and E. L. Muetterties, *J. Amer. Chem. Soc.*, 93, 1797 (1971).

(27) R. W. Baker and P. Pauling, *Chem. Commun.*, 1495 (1969), reported a near-regular MP_4 tetrahedron for $HRh[P(C_6H_5)_3]_4$.

(28) R. W. Baker, B. Ilmaier, P. J. Pauling, and R. S. Nyholm, *ibid.*, 1077 (1970), found an ML_4 tetrahedral substructure for $HRh[P(C_6H_5)_3]_3As(C_6H_5)_3$.

(29) B. A. Frenz and J. A. Ibers, *Inorg. Chem.*, **9**, 2403 (1970), found the CoP_4 substructure to closely approach regular tetrahedral in $HCo(PF_3)_4$.

(30) K. C. Dewhirst, W. Keim, and C. A. Reilly, *ibid.*, 7, 546 (1968), report a quintet of doublets for $HRh[P(CH_3)(C_6H_5)_2]_4$ at $-60°$ and proposed a C_{4v} square-pyramidal form. We believe that the spectrum observed by them is simply the limiting high-temperature spectrum for a nonrigid C_{3v} form.

(31) G. M. Whitesides and H. L. Mitchell, *J. Amer. Chem. Soc.*, **91**, 5384 (1969).

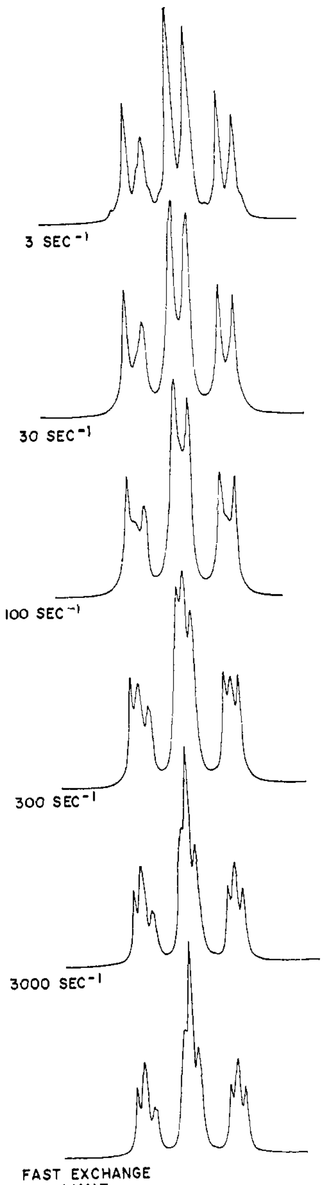

Figure 9. Calculated 220-MHz nmr spectra of $FeH_2[P(OC_2H_5)_3]_4$ at several exchange rates for basic permutational set II using the complete treatment. The fast-exchange-limit spectrum is calculated directly from the effective fast-exchange-limit Hamiltonian. T_2 = 0.05 sec.

not be found again and the indices i and j and the values of the I_{ij}^- are then used to calculate the contribution of these transitions to the spectrum using eq 1, 2, and 4. The program then continues to search the $I_z = -I$, $I_z = -I + 1$ block of I^- for new nonzero elements and the procedure outlined above is repeated until all the $I_z = -I, I_z = -I + 1$ transitions have been found. At this stage the $I_z = -I + 2$ block of the Hamiltonian is set up and the whole procedure is repeated until finally the $I_z = I$ block is reached and the calculation is complete. The calculation of a spectrum consisting of some 500–1000 points takes about 45 sec for the non-noise-decoupled ^{31}P spectra and about 30 sec for the ^1H spectra on a Univac 1108 for mechanisms I, III, and IV. For mechanism II, there is much more symmetry factoring and the calculation is faster. In the case of the proton spectra, the largest complex matrices that have to be diagonalized are of dimension 20 × 20 for mechanisms III and IV, 12 × 12 for mechanism I, and only 4 × 4 for mechanism II (see Figure 9).

A general computer program has also been written for the case of nonmutual intramolecular exchange, and this program employs a similar numerical factoring procedure.

Appendix II. Symmetry Considerations

Theorem. If the Hamiltonian H_0 is invariant under the transformations T_i and T_j in the appropriate Hilbert space, then the Liouville operator $\mathcal{L}_0$ corresponding to H_0 is invariant to the direct products of T_i and T_j^* in the corresponding Liouville space; *i.e.*, if $T_i^{-1}H_0T_i = H_0$ and $T_j^{-1}H_0T_j = H_0$, then

$$(T_i \otimes T_j^*)^{-1}\mathcal{L}_0(T_i \otimes T_j^*) = \mathcal{L}_0$$

$$(T_j \otimes T_i^*)^{-1}\mathcal{L}_0(T_j \otimes T_i^*) = \mathcal{L}_0$$

Proof. From eq 1 and 2 the Liouville operator is proportional to $(H_0 \otimes E^* - E \otimes H_0^*)$,[21] where E is the unit matrix and

$$\begin{aligned}(T_i \otimes T_j^*)^{-1}(H_0 \otimes E^* - E \otimes H_0^*)(T_i \otimes T_j^*) &= \\ (T_i^{-1} \otimes T_j^{*-1})(H_0T_i \otimes E^*T_j^* - ET_i \otimes H_0^*T_j^*) &= \\ (T_i^{-1}H_0T_i \otimes T_j^{*-1}E^*T_j^* - T_i^{-1}ET_i \otimes T_j^{*-1}H_0^*T_j^*) &= \\ (H_0 \otimes E^* - E \otimes H_0^*)&\end{aligned}$$

and the proof for the invariance of $\mathcal{L}_0$ to $(T_j \otimes T_i^*)$ is identical. This result is an extension of theorem 3 of Kleier and Binsch.[19]

Thus, if the high-resolution nmr Hamiltonian is invariant to the operators of the group G, then the Liouville operator is invariant to the direct products of these operators with their complex conjugates which form a group $G \otimes G^*$.

In our case the Hamiltonian belongs to the Abelian group C_{2v}. The elements of C_{2v} are their own complex conjugates so that $G \otimes G^* = C_{2v} \otimes C_{2v}$. The character table is shown in Table I, and further discussion is restricted to the group C_{2v}.

In the necessary symmetrized basis in which the Hamiltonian and the Liouville operator are diagonal, the density matrix basis elements corresponding to the allowed transition belong to the irreducible representations A_1A_1, A_2A_2, B_1B_1, and B_2B_2 of $C_{2v} \otimes C_{2v}$, corresponding to the A_1, A_2, B_1, and B_2 transitions of C_{2v}.

The exchange term can be written

$$\begin{aligned}\sum_i \chi_i = (E \otimes E)(\chi_1)(E \otimes E) + \\ (C_2 \otimes C_2)(\chi_1)(C_2 \otimes C_2) + (\sigma_v \otimes \sigma_v)(\chi_1)(\sigma_v \otimes \sigma_v) + \\ (\sigma_v' \otimes \sigma_v')(\chi_1)(\sigma_v' \otimes \sigma_v')\end{aligned}$$

Consider now the transformation with $C_2 \otimes C_2$

$$\begin{aligned}\sum_i \chi_i' = (C_2 \otimes C_2)(E \otimes E)(\chi_1)(E \otimes E)(C_2 \otimes C_2) + \\ (C_2 \otimes C_2)(C_2 \otimes C_2)(\chi_1)(C_2 \otimes C_2)(C_2 \otimes C_2) + \\ (C_2 \otimes C_2)(\sigma_v \otimes \sigma_v)(\chi_1)(\sigma_v \otimes \sigma_v)(C_2 \otimes C_2) + \\ (C_2 \otimes C_2)(\sigma_v' \otimes \sigma_v')(\chi_1)(\sigma_v' \otimes \sigma_v')(C_2 \otimes C_2) = \\ (C_2 \otimes C_2)(\chi_1)(C_2 \otimes C_2) + (E \otimes E)(\chi_1)(E \otimes E) + \\ (\sigma_v' \otimes \sigma_v')(\chi_1)(\sigma_v' \otimes \sigma_v') + (\sigma_v \otimes \sigma_v)(\chi_1)(\sigma_v \otimes \sigma_v)\end{aligned}$$

Table I. The Character Table for the Group $C_{2v}\otimes C_{2v}$

	$E\otimes$				$C_2\otimes$				$\sigma_v\otimes$				$\sigma_v'\otimes$			
$C_{2v}\otimes C_{2v}$	E	C_2	σ_v	σ_v'	E	C_2	σ_v	σ_v'	E	C_2	σ_v	σ_v'	E	C_2	σ_v	σ_v'
A_1A_1	1	1	1	1	1	1	1	1	1	1	1	1	1	1	1	1
A_1A_2	1	1	−1	−1	1	1	−1	−1	1	1	−1	−1	1	1	−1	−1
A_1B_1	1	−1	1	−1	1	−1	1	−1	1	−1	1	−1	1	−1	1	−1
A_1B_2	1	−1	−1	1	1	−1	−1	1	1	−1	−1	1	1	−1	−1	1
A_2A_1	1	1	1	1	1	1	1	1	−1	−1	−1	−1	−1	−1	−1	−1
A_2A_2	1	1	−1	−1	1	1	−1	−1	−1	−1	1	1	−1	−1	1	1
A_2B_1	1	−1	1	−1	1	−1	1	−1	−1	1	−1	1	−1	1	−1	1
A_2B_2	1	−1	−1	1	1	−1	−1	1	−1	1	1	−1	−1	1	1	−1
B_1A_1	1	1	1	1	−1	−1	−1	−1	1	1	1	1	−1	−1	−1	−1
B_1A_2	1	1	−1	−1	−1	−1	1	1	1	1	−1	−1	−1	−1	1	1
B_1B_1	1	−1	1	−1	−1	1	−1	1	1	−1	1	−1	−1	1	−1	1
B_1B_2	1	−1	−1	1	−1	1	1	−1	1	−1	−1	1	−1	1	1	−1
B_2A_1	1	1	1	1	−1	−1	−1	−1	−1	−1	−1	−1	1	1	1	1
B_2A_2	1	1	−1	−1	−1	−1	1	1	−1	−1	1	1	1	1	−1	−1
B_2B_1	1	−1	1	−1	−1	1	−1	1	−1	1	−1	1	1	−1	1	−1
B_2B_2	1	−1	−1	1	−1	1	1	−1	−1	1	1	−1	1	−1	−1	1

thus $\Sigma_i\chi_i$ is clearly invariant to $C_2\otimes C_2$ and the invariance to $(E\otimes E)$, $(\sigma_v\otimes\sigma_v)$, and $(\sigma_v'\otimes\sigma_v')$ follows similarly.

Now consider the transformation $(C_2\otimes E)$

$$\begin{aligned}\sum_i\chi_i' = {} & (C_2\otimes E)(E\otimes E)(\chi_1)(E\otimes E)(C_2\otimes E) + \\ & (C_2\otimes E)(C_2\otimes C_2)(\chi_1)(C_2\otimes C_2)(C_2\otimes E) + \\ & (C_2\otimes E)(\sigma_v\otimes\sigma_v)(\chi_1)(\sigma_v\otimes\sigma_v)(C_2\otimes E) + \\ & (C_2\otimes E)(\sigma_v'\otimes\sigma_v')(\chi_1)(\sigma_v'\otimes\sigma_v')(C_2\otimes E) = \\ & (C_2\otimes E)(\chi_1)(C_2\otimes E) + (E\otimes C_2)(\chi_1)(E\otimes C_2) + \\ & (\sigma_v'\otimes\sigma_v)(\chi_1)(\sigma_v'\otimes\sigma_v) + (\sigma_v\otimes\sigma_v')(\chi_1)(\sigma_v\otimes\sigma_v')\end{aligned}$$

and hence $\Sigma_i\chi_i$ is not necessarily invariant to $(C_2\otimes E)$.

In general, we have the result that $\Sigma_i\chi_i$ is invariant to the group elements $G_i\otimes G_i$ but not necessarily to the $G_i\otimes G_j$, $i \neq j$; consequently, $\Sigma_i\chi_i$ contains parts transforming as the A_1A_1, A_2,A_2, B_1B_1, and B_2B_2, irreducible representations of $C_{2v}\otimes C_{2v}$. Thus, the exchange process has matrix elements connecting the density-matrix basis elements corresponding to allowed transitions of different symmetry types but does not connect density-matrix basis elements corresponding to allowed transitions with those corresponding to forbidden transitions.

Further factoring will depend on the detailed nature of χ_1. For example, in mechanism II, the permutation P_1 is invariant to all elements of C_{2v} and the exchange matrix χ_1 is invariant to all elements of $C_{2v}\otimes C_{2v}$. Consequently, $\Sigma_i\chi_i$ belongs to the A_1A_1 irreducible representation and the exchange process does not connect density-matrix elements corresponding to transitions of different symmetry types. On this basis we expect that the largest matrix that will have to be diagonalized will be of dimension 12 × 12, corresponding to the 12 A_1 transitions

$$I_z = 0 \rightarrow 1 \qquad I_{z_H} = 0 \rightarrow 1$$

and the 12 A_1 transitions

$$I_z = -1 \rightarrow 0 \qquad I_{z_H} = -1 \rightarrow 0$$

This corresponds to an upper limit and, in fact, the largest matrices that need to be diagonalized in this case are of dimension 4 × 4. The calculated spectra are shown in Figure 9. One of the basic permutational sets corresponding to case II is the single permutation (56) which exchanges the two hydrogens. The additional factoring can be explained in terms of the invariance of the $I_{z_H} = \pm 1$ functions to proton exchange. For example, the 12 A_1 $I_z = -1 \rightarrow 0$, $I_{z_H} = -1 \rightarrow 0$ transitions occur between the three A_1 $I_z = -1$, $I_{z_H} = -1$ states and the four A_1 $I_z = 0$, $I_{z_H} = 0$ states. Thus the invariance of the $I_{z_H} = 1$ states to proton exchange results in a further factoring to three 4 × 4 complex non-Hermitian matrices. This additional factoring was not anticipated but was nevertheless realized by the numerical factoring procedure.

The method outlined above can readily be extended to groups other than C_{2v}.